

Resonance Light Scattering and Its Application in Determining the Size, Shape, and Aggregation Number for Supramolecular Assemblies of Chromophores

Peter J. Collings,^{*,†} Esther J. Gibbs,[‡] Tammy E. Starr,[‡] Oskar Vafek,[‡] Cyril Yee,[§] Laura A. Pomerance,[†] and Robert F. Pasternack[§]

Department of Physics and Astronomy, Swarthmore College, Swarthmore, Pennsylvania 19081; Department of Chemistry, Goucher College, Towson, Maryland 21204; and Department of Chemistry, Swarthmore College, Swarthmore, Pennsylvania 19081

Received: May 19, 1999

Resonance light scattering (RLS) on supramolecular assemblies of chromophores is a sensitive and selective method to extract size and shape information, but the interpretation of the data is complicated by the large amount of absorption present. By combining extinction and RLS measurements on the same samples of acidified tetrakis(4-sulfonatophenyl)porphine (H₄TPPS), a technique is described whereby the scattering spectrum can be “corrected” for absorption. An additional benefit of this analysis is that the spectrum obtained for these solutions on a spectrophotometer, which is really an extinction spectrum, can be parsed into its absorption and scattering components. The results demonstrate that scattering contributes significantly to the aggregate peak in the extinction spectrum. Knowledge of the absorption and scattering components allows an estimation of the average aggregation number to be made, which for these solutions is on the order of 10⁵–10⁶. In addition, static and dynamic light scattering measurements provide evidence for a rodlike aggregate with about 10 000 molecules along its length and about 20 molecules across its diameter.

1. Introduction

Recent studies have shown resonance light scattering (RLS) to be a valuable technique for detecting and characterizing extended aggregates of chromophores.^{1–3} The scattering intensity of such species is enhanced by *several orders of magnitude* at or near the wavelength of absorption when strong electronic coupling exists among the chromophore units. As a result, RLS is an extremely sensitive and selective technique for monitoring such molecular assemblies and shows promise for determining their size and shape as well.^{4,5} In this paper, we present results from RLS experiments using both an ordinary computer-controlled spectrofluorimeter in which the scattering angle is fixed at 90° and a laser light scattering apparatus in which the scattering angle is variable. A computational strategy that uses these data to estimate the average number of monomers in an aggregate is also presented.

Unlike conventional light scattering techniques in which the wavelength region of chromophore absorption is avoided, RLS measurements focus on this portion of the electromagnetic spectrum. Therefore, similar to the corrections needed in fluorescence spectroscopy for primary and secondary absorption processes, RLS spectra need to be corrected for absorption of the incident and the scattered light. This paper presents an empirical method for making absorption corrections of RLS spectra obtained on fluorescence spectrometers with right angle detection. Obtaining the required absorption data to carry out this correction is not as straightforward as in fluorescence spectroscopy, but is absolutely crucial in order to extract useful information from spectroscopy experiments on aggregates of

chromophores. The additional complication encountered here arises because, in a spectrophotometric experiment on solutions that scatter appreciable light, it is the *extinction* that is measured and not absorption. Therefore, consideration must be given both to the absorption of the sample and also to the scattering which removes photons from the incident and scattered beams. Thus, in developing a method for the correction of RLS spectra for both absorption and scattering, a procedure for separating the extinction measurement into its components is required. What follows is an outline of the procedures for (i) finding the “effective” path length over which absorption and scattering act in a sample, (ii) separating an extinction measurement into its absorption and scattering components while simultaneously correcting RLS spectra for absorption, and (iii) using the absorption and scattering components to estimate the average number of monomers in an aggregate. The results from this last technique are then compared to the determination of aggregate size obtained from RLS experiments in which the scattering angle is varied, and dynamic RLS experiments in which the time autocorrelation function of the scattered light is measured.

2. Experimental Section

2.1. Chemicals and Solution Preparation. The porphyrin tetrakis(4-sulfonatophenyl)porphine (H₂TPPS, Figure 1) was obtained from MidCentury Chemical (Posen, IL) as the tetrasodium salt. (The charges of porphyrin species are not shown explicitly for the sake of convenience.) The polystyrene spheres used in these studies were obtained from Seradyn, Inc. (Indianapolis, IN). Stock porphyrin solutions (200 μM range) were stored in the dark and used within five days of preparation. The stock was filtered with 0.1 μm filters just prior to dilution for spectral measurements. Diluted porphyrin solutions (μM range) were used within 12 h unless otherwise noted. The

* Corresponding author. E-mail: pcollin1@swarthmore.edu. Fax: 610-328-7895.

† Department of Physics and Astronomy, Swarthmore College.

‡ Goucher College.

§ Department of Chemistry, Swarthmore College.

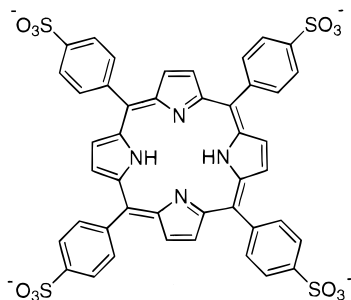


Figure 1. Structure of tetrakis(4-sulfonatophenyl)porphyrin (H_2TPPS).

concentrations of porphyrin solutions were determined in 1 mM phosphate buffer at pH 6.8 using a value for the molar absorptivity of $\epsilon = 5.53 \times 10^5 \text{ M}^{-1} \text{ cm}^{-1}$ at 413 nm.⁶ All solutions and suspensions were prepared using Millipore purified water that had been previously filtered with a 0.1 μm filter to remove any particulates. All other chemicals were reagent grade, purchased from Fisher Scientific, and used without further purification.

Aggregation of this water-soluble porphyrin to form J-aggregates having large RLS intensity occurs at low pH conditions (when the porphyrin is in its diacid form). Since the characteristics of these aggregates depend on the protocol used to make the solutions, different methods were investigated in search of approaches that consistently gave reproducible results. This criterion was met if the solutions were prepared by the addition of a concentrated stock solution of H_2TPPS at neutral pH to a solution of HCl at pH 1. In addition, the concentration of H_2TPPS was kept low (below 4 μM) for two reasons: (1) to keep the magnitude of the correction due to absorption at a significant but not overwhelmingly dominant level, and (2) to minimize complexities in the aggregate structure that may occur at high concentrations (e.g., the formation of higher order mesostructure assemblies). As a result, all of the solutions studied had significant amounts of H_4TPPS in the monomer form. Solutions were allowed to equilibrate for several hours before measurements were made.

2.2. Instrumentation and Equipment. Extinction measurements were conducted on a JASCO V550 spectrophotometer using Fisher polymethacrylate cuvettes (1 cm path length). Porphyrin staining of the cuvette surface is less severe for polymethacrylate than for quartz.

Resonance light scattering measurements were conducted on two fluorimeters: a SPEX Fluorolog spectrofluorimeter (fluorimeter no. 1), as previously described¹⁻³ and the updated version of this fluorimeter, a Fluorolog 3, now built by Instruments S.A., Inc. (fluorimeter no. 2). For both instruments, RLS spectra were obtained using the ratio mode for signal intensity and in the synchronous scanning mode in which the emission and excitation monochromators are preset to identical wavelengths.

Scattering intensities were also measured using an Innova-70 mixed gas laser with a Brookhaven Instruments BI-9000AT light scattering system. Cylindrical glass sample containers with a diameter of 2.54 cm were employed. Band-pass filters were placed in front of the detector to minimize the contamination from fluorescent light, which for H_4TPPS is emitted at significantly longer wavelengths. Scattering intensities at a single wavelength and at a single angle were measured multiple times (typically between 3 and 8 times) with the average of these values used in the analysis.

2.3. Methods To Correct Scattering Intensities for Absorption. The correction of incident and scattered light intensities

due to absorption effects is essential for any quantitative application of the RLS technique. The correction of the RLS intensity is analogous to corrections of fluorescence spectra for primary and secondary inner filtering. Computational methods for carrying out these corrections are well documented in the literature.^{7,8} As applied to scattering spectra where the incident and scattered wavelengths are identical, the attenuation of the RLS intensity due to absorption can be taken into account using the following correction factor:

$$F^{\text{corr}}(\lambda) = \frac{5.3038 A^2 (x_2 - x_1)(y_2 - y_1)}{(10^{-Ax_1} - 10^{-Ax_2})(10^{-Ay_1} - 10^{-Ay_2})} \quad (1)$$

A is the absorption/cm of the solution at a given wavelength and (x_1, x_2) and (y_1, y_2) are the positions of the ends of the interrogation zone for the incident and scattered beam, respectively. The interrogation zone is the region of sample through which both incident light passes and scattered light reaches the detector. The difficulty of accurately measuring the dimensions of the interrogation zone makes this method impractical.

In an empirical method developed here, the correction factor can be written in the form

$$F^{\text{emp}}(\lambda) = 10^{AL_{\text{eff}}} \quad (2)$$

which uses an experimentally determined effective path length, L_{eff} , to approximate the average distance the incident and scattered light travels through the sample. The effective path length in the correction factor is obtained by measuring scattering spectra for solutions containing nonabsorbing scatterers in the presence and absence of nonscattering absorbers. Then, if I is the intensity of the scattered light at a given wavelength

$$\frac{I_{\text{scatterer w/absorber}}}{I_{\text{scatterer w/o absorber}}} = 10^{-AL_{\text{eff}}} \quad (3)$$

where A is the absorbance/cm of the nonscattering absorbers at the wavelength under consideration. The above ratio of scattered intensities is plotted against absorbance and a least-squares fitting program is used to find the best value of the effective path length. For these experiments, suspensions of polystyrene spheres (diameter = 0.065 μm) and potassium dichromate at pH 3 were used as the nonabsorbing scatterers (in the wavelength range monitored) and the nonscattering absorbers, respectively.

Laser scattering experiments were conducted to confirm the assumption that the potassium dichromate solutions did not contribute any additional scattering beyond background from the aqueous solvent. Unlike a conventional fluorimeter, accurate measurement of the actual path length of the incident and scattered light is relatively simple for the laser instrumentation. The sample containers are cylindrical and the incident beam and detection path are extremely narrow. Therefore, to a good approximation the actual path length for the laser system is the inside diameter of the cylindrical sample holder (2.52 cm).

3. Results and Discussion

3.1. Determination of the Effective Path Length. Scattering experiments were conducted on solutions of potassium dichromate using the laser scattering instrumentation. "Off-resonance" scattering measurements were first performed for solvent and potassium dichromate solutions at 568 nm. At all concentrations of potassium dichromate (with concentration monitored by

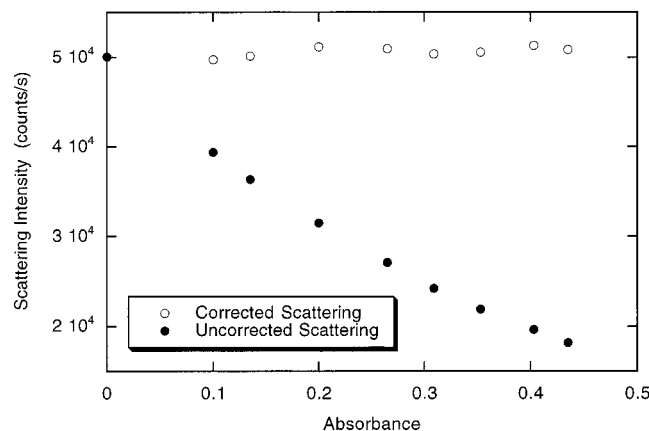


Figure 2. Scattering intensity (90° , laser instrument) at 454.4 nm versus absorbance at 454 nm for solutions with different concentrations of potassium dichromate: (●) actual data; (○) actual data corrected for absorption using eq no. 2.

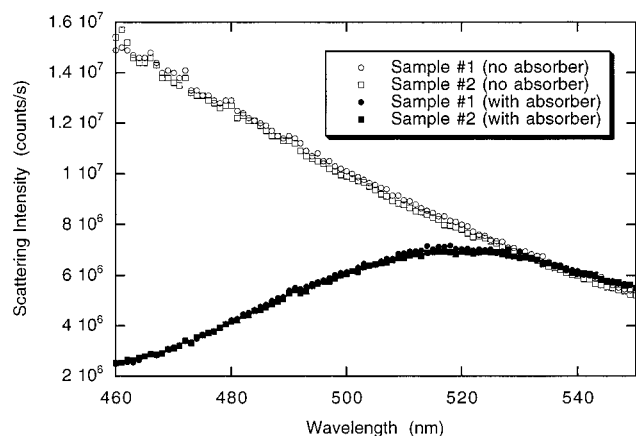


Figure 3. Scattering spectra (90° , fluorimeter no. 1) for two suspensions of $0.065 \mu\text{m}$ diameter polystyrene spheres with and without potassium dichromate: (unfilled symbols) no potassium dichromate; (filled symbols) with potassium dichromate.

absorbance of the solution at 454 nm), there was no additional scattering above the amount observed for the solvent alone.

“On-resonance” scattering of the potassium dichromate solutions was measured at 454.4 nm. Shown in Figure 2 is the “on-resonance” scattering for these solutions. The “on-resonance” scattering is observed to decrease from the background scattering level as the absorbance of the potassium dichromate solutions increases. The scattering of these solutions corrected for absorption was determined using the empirical correction factor given in eq 2 and a value of 2.52 cm for the actual path length of the laser cell. Within experimental error for all eight solutions, the scattering intensities corrected for absorption are identical to the background values obtained at zero absorbance (no potassium dichromate). These results lend support for the following conclusions: (i) potassium dichromate, under the conditions of these experiments, is a “nonscattering” absorber, and (ii) the empirical correction factor technique is valid.

In order to use the empirical correction factor on spectra obtained with a fluorimeter, the effective path length, L_{eff} , for the fluorimeter must be determined. This was done by measuring the absorption of potassium dichromate solutions and the scattering from suspensions of polystyrene spheres with and without the added (nonscattering) potassium dichromate absorbers. Shown in Figure 3 are the scattering spectra obtained for

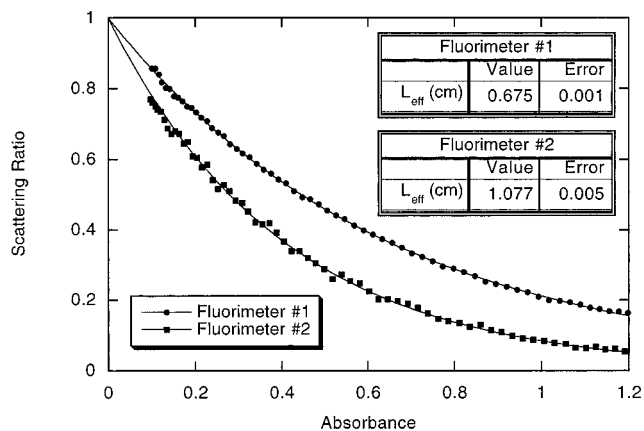


Figure 4. Ratio of the scattering intensities from one of the samples of Figure 3 as a function of absorbance (fluorimeter no. 1) along with similar data for fluorimeter no. 2. The curves represent least-squares fits using eq 3.

suspensions of $0.065 \mu\text{m}$ polystyrene spheres in the presence and absence of dissolved potassium dichromate for fluorimeter no. 1.

The scattering of the polystyrene spheres alone decreases with increasing wavelength, a profile typical of Rayleigh scattering. In the presence of the potassium dichromate absorbers, the scattering from the polystyrene spheres is reduced throughout most of the wavelength region shown. At wavelengths greater than about 540 nm, the polystyrene sphere scattering with and without potassium dichromate is about the same. The potassium dichromate absorbance is so small in this wavelength region (less than 0.05) that it has very little effect on the scattering from the polystyrene spheres.

Shown in Figure 4 is a plot of the scattering ratio (the scattering intensity of the polystyrene spheres with potassium dichromate divided by the scattering intensity of the polystyrene spheres without potassium dichromate) versus the absorption of a potassium dichromate solution of the same concentration but with no polystyrene spheres. Each point of the plot represents data obtained at a different wavelength. Least-squares fits to eq 3 are also shown in the figure. As evident from Figure 4, the least-squares fits to eq 3 over an absorbance range from 0.1 to 1.2 are quite good and yield effective path lengths of $0.675 \pm 0.001 \text{ cm}$ for fluorimeter no. 1 and $1.077 \pm 0.005 \text{ cm}$ for fluorimeter no. 2. Direct observation of where the incident light strikes the sample cuvette confirmed that the optical paths in these two fluorimeters are significantly different. This demonstrates just how crucial it is to determine L_{eff} for each fluorimeter, even when the models are the same.

For fluorimeter no. 2, data for three suspensions of polystyrene spheres, each containing different concentrations of potassium dichromate, were combined for analysis. In addition, data were collected using three slit widths (0.1, 0.15, and 0.25 mm). When the data for the three concentrations and the three slit widths were analyzed independently, the values obtained for L_{eff} ranged from 1.07 to 1.09 cm with an average value of 1.08 cm. Although the fits were quite good, an additional check for any significant variation in the effective path length with wavelength was conducted. A series of six preparations of polystyrene spheres with and without varying amounts of potassium dichromate were monitored on fluorimeter no. 2. The data were analyzed for determination of L_{eff} at three wavelengths (430, 454, and 490 nm) and at three different slit widths. The range of L_{eff} values was 1.07–1.10 cm with an average value of 1.08 cm.

3.2. Separation of an Extinction Spectrum into Absorption and Scattering Components While Correcting the Scattering Spectrum for Absorption. In the course of our experimental studies, it became apparent that in many cases extinction spectra of porphyrin aggregates contain a significant scattering component. Thus, what is really desired is not only a method to find the “true” scattering spectra at a fixed angle (fluorimeter data), but also a method to separate the absorption and scattering components of the extinction spectra (spectrophotometer data). There is a connection between the “true” scattering data from the fluorimeter and the scattering component of the extinction data from the spectrophotometer, since the former measures the scattering at a fixed angle whereas the latter measures the total amount of scattering at all angles. The key to separating the extinction spectra into its components is to make use of this connection.

Measuring spectra of a suspension of polystyrene spheres using both a spectrophotometer and a fluorimeter yields “true” scattering information in both cases since polystyrene spheres do not absorb in the region of interest. If this is done for different scattering intensities (different suspension densities of polystyrene spheres), the quantitative connection between these two measurements becomes known as a function of both scattering intensity and wavelength. For any sample that scatters light with the same angular dependence as the polystyrene spheres, therefore, measurement of the scattering spectrum using the fluorimeter (corrected for the absorption component only) yields the scattering component of the extinction spectrum. Since the absorption component needed for the correction is the extinction spectrum corrected for the scattering component (absorption = extinction – scattering), a self-consistent equation results in which the absorption component is the only unknown. Solving this equation at a given wavelength yields the absorption component; subtraction of the absorption component from the extinction yields the scattering component. Finally, correction of the fluorimeter data using the absorption component and the effective path length yields the “true” 90° scattering intensity. If this procedure is repeated for each wavelength of the extinction spectrum, the “true” absorption spectrum and scattering spectrum are obtained. However, since the scattered light from the polystyrene spheres and the sample being studied do not necessarily have the same angular distribution (their structure factors are likely to differ), angle-dependent light scattering experiments should be done on both to obtain this information. Once this has been accomplished, an appropriate factor taking this difference into account can be included in the self-consistent equation before it is solved.

The various steps are illustrated below using 0.204 μm diameter polystyrene spheres and solutions of acidified tetrakis-(4-sulfonatophenyl)porphine, H₄TPPS, containing both monomers and aggregates. First, an extinction spectrum using the spectrophotometer, a scattering spectrum (in this case using fluorimeter no. 2), and angular scattering data using the laser apparatus are obtained for the porphyrin solution. Second, a series of polystyrene sphere suspensions is prepared that represent the range of “true” scattering anticipated from the porphyrin solution. Third, extinction spectra and fluorimeter scattering spectra are obtained for each polystyrene suspension. Finally, the angular scattering data are obtained for one (or more) of the polystyrene suspensions.

Plots at each wavelength are made of the fluorimeter scattering versus extinction for the polystyrene spheres. Some of these are shown in Figure 5, where it is clear that they are fairly linear but with a small amount of downward curvature.

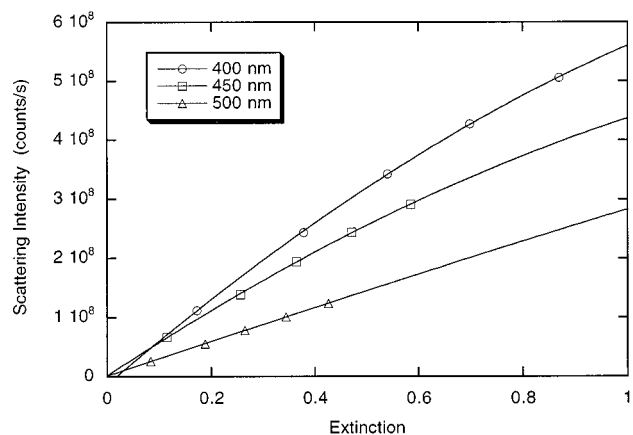


Figure 5. Scattering intensity (90°) versus extinction at three different wavelengths for five different suspensions of 0.204 μm diameter polystyrene spheres. The curves represent least-squares quadratic fits.

Least-squares fits to a quadratic function are made at each wavelength, establishing the quantitative connection between scattering as measured in the fluorimeter and scattering as measured in the spectrophotometer:

$$I_{\text{spheres}} = aS_{\text{spheres}}^2 + bS_{\text{spheres}} + c \quad (4)$$

I_{spheres} is the scattering intensity measured in the fluorimeter, S_{spheres} is the scattering component as measured in the spectrophotometer ($S_{\text{spheres}} = E_{\text{spheres}} =$ extinction for these nonabsorbing scatterers), and a , b , and c are the coefficients as determined by the least-squares quadratic fit.

The angular dependence of the light scattering for both a suspension of 0.204 μm diameter polystyrene spheres and the H₄TPPS solution is shown in Figure 6. To account for the difference in the angular distributions, the ratio of the amount of light scattered at 90° to the total amount of light scattered at all angles is found for each sample. The latter is simply the integral of the data shown in Figure 6 if the data is multiplied by the sine of the scattering angle before integration. If $I(\theta)$ is the intensity of light scattered at angle θ , then the ratio is given by

$$r = \frac{I(90^\circ)}{\int_0^{180^\circ} I(\theta) \sin \theta d\theta} \quad (5)$$

The self-consistent equation relating the spectrophotometer and fluorimeter data at a specific wavelength can now be written. The left-hand side of the equation is the scattering intensity of the H₄TPPS solution from the fluorimeter, I_{sample} , corrected for absorption. The right-hand side of the equation is a determination of the fluorimeter scattering intensity using the connection between the spectrophotometer and fluorimeter data as obtained from the analysis using the suspensions of polystyrene spheres. The extinction of the H₄TPPS solution, E_{sample} , appears on the right-hand side. Finally, the ratios describing the different angular distributions of scattered light, r_{sample} and r_{spheres} , must be present in appropriate places. The self-consistent equation in which the only unknown is the absorption component of the H₄TPPS solution, A_{sample} , is therefore

$$I_{\text{sample}} 10^{A_{\text{sample}} L_{\text{eff}}} = \frac{r_{\text{sample}}}{r_{\text{spheres}}} [a(E_{\text{sample}} - A_{\text{sample}})^2 + b(E_{\text{sample}} - A_{\text{sample}}) + c] \quad (6)$$

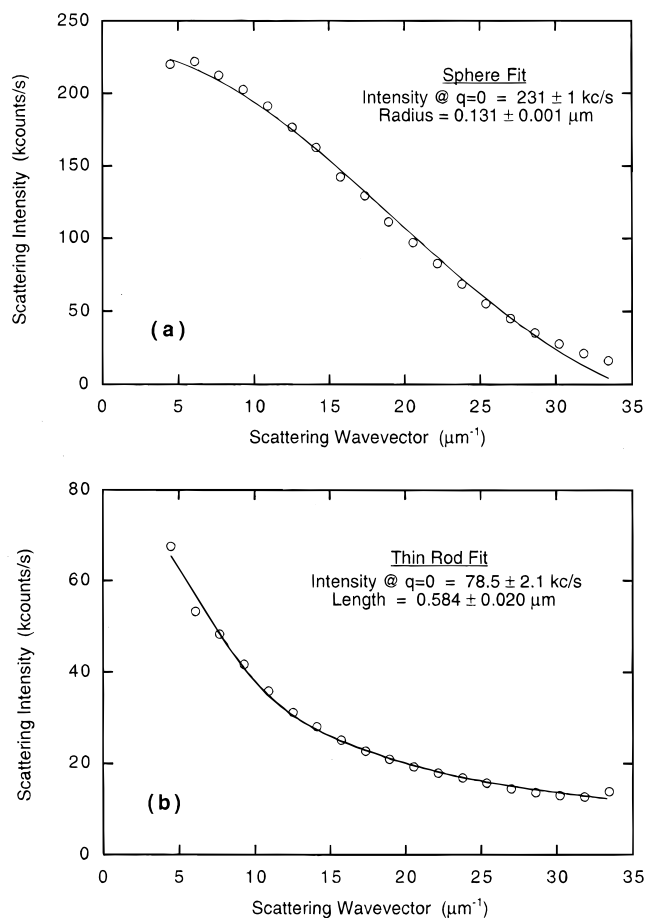


Figure 6. Scattering wavevector dependence of the scattering intensity at 488 nm for (a) a suspension of 0.204 μm diameter polystyrene spheres and (b) a 3.71 μM solution of H_4TPPS . The curves represent a least-squares fit to the scattering function for (a) a sphere and (b) a thin rod.

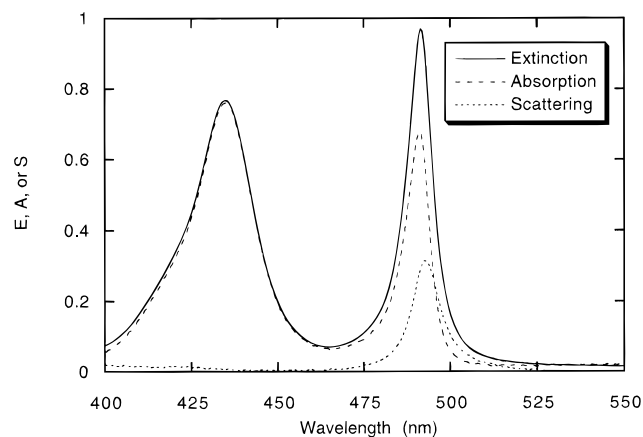


Figure 7. Extinction spectrum for a 3.71 μM solution of H_4TPPS , showing its absorption and scattering components.

The result of solving this self-consistent equation at 0.5 nm intervals for a 3.71 μM H_4TPPS solution is shown in Figure 7. Notice that a significant part of the extinction in the region of the aggregate peak (489 nm), over 50% at some wavelengths, is due to scattering. Another striking feature in this part of the spectrum is that the absorption and scattering components do not have their maxima at exactly the same wavelength, but instead the scattering component peak is red-shifted by 2 nm relative to the absorption component peak. Finally, notice that there is no scattering component due to the monomers in solution (435 nm). Rather, the small scattering component at

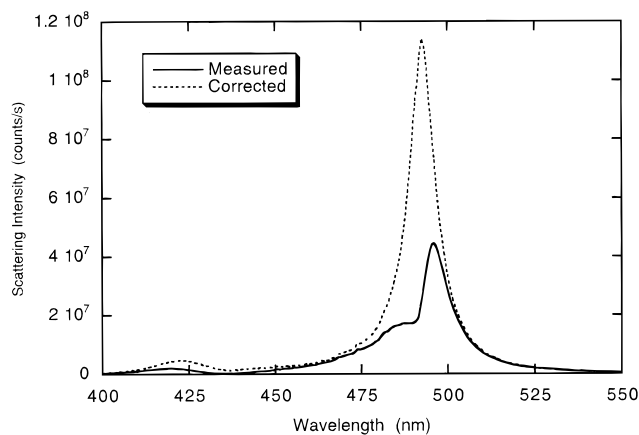


Figure 8. Scattering spectrum for a 3.71 μM solution of H_4TPPS : (solid line) actual data; (dashed line) actual data corrected for absorption.

shorter wavelengths simply reflects the nonresonant (Rayleigh) scattering from the H_4TPPS aggregates.

The “true” scattering spectrum is given by the left-hand side of the self-consistent equation and can be calculated once the absorption and scattering components of the extinction spectrum are known. Both the original and corrected fluorimeter spectra are shown in Figure 8. Notice (1) that the decreased scattering around 435 nm due to absorption by monomers all but disappears in the corrected spectrum, (2) that the scattering in the vicinity of the aggregate peak (489 nm) is much enhanced in the corrected spectrum since the effects of absorption are no longer present, and (3) that the difference in wavelength between the absorption and scattering peaks is clearly revealed by the asymmetry of the uncorrected spectrum in the vicinity of the scattering peak.

The small peak around 425 nm raises an interesting question. There is evidence that H_4TPPS forms H aggregates also, with a peak extinction blue-shifted to about 420 nm.^{9,10} On the other hand, the minimum in the intensity around 435 nm in the uncorrected spectrum is surely due to absorption of incident and scattered light by monomers in solution. The procedure used to correct for absorption should eliminate this effect, but clearly a small minimum remains in the corrected spectrum. Whether the correction is not perfect or scattering from H-aggregates (or both) affect the corrected scattering spectrum is an open question.

3.3. Estimation of the Average Number of Monomers in an Aggregate. Knowing the absorption and scattering components of the extinction spectrum allows for an estimation of the average number of monomers in an aggregate. To simplify the calculation, the assumption is made that the size of the aggregates is much smaller than the wavelength of light and therefore the relationships governing Rayleigh scattering are applicable. However, as will be seen from the analysis of these results, it is evident that at least one dimension of the aggregates with which we are working is greater than the wavelength of light. So this calculation should be viewed as an order of magnitude estimation, although it might be more accurate than it at first seems should two of the dimensions of the aggregates be much smaller than the wavelength of light (i.e., the aggregates are long and thin).

If the concentration of aggregates, c_A , is known, it is possible to determine the absorption, scattering, and extinction coefficients a_A , s_A , and e_A , respectively,

$$a_A = \frac{A_A}{c_A L} \quad s_A = \frac{S_A}{c_A L} \quad e_A = \frac{E_A}{c_A L} \quad (7)$$

TABLE 1: Size and Shape Estimates for Four H₄TPPS Solutions^a

concn (μM)	aggregn no.	length (μm)	hydrodyn radius (μm)
2.33	~610 000	0.86 ± 0.06	0.23 ± 0.11
2.79	~550 000	0.66 ± 0.03	0.21 ± 0.09
3.25	~400 000	0.63 ± 0.02	0.18 ± 0.09
3.71	~320 000	0.58 ± 0.06	0.17 ± 0.08

^a The length and hydrodynamic radius are determined from angular light scattering and dynamic light scattering experiments, respectively.

where L is the cell path length of the spectrophotometer (usually 1 cm). A_A , S_A , and E_A are the absorption component, scattering component, and extinction, respectively, at the wavelength of maximum scattering component for the aggregate (about 489 nm). It is difficult to determine c_A , but it is not difficult to determine the concentration of porphyrin in aggregate form, c_A^* , which can be determined from subtracting the concentration of monomers from the total porphyrin concentration. These last two are known from the molar absorptivities of the monomer in its free base and diacid forms. So absorption, scattering, and extinction coefficients can be determined for the porphyrin units in aggregate form

$$a_A^* = \frac{A_A}{c_A^* L} \quad s_A^* = \frac{S_A}{c_A^* L} \quad e_A^* = \frac{E_A}{c_A^* L} \quad (8)$$

If there are N monomers in each aggregate, then $c_A^* = Nc_A$ and expressions for the absorption and scattering components assuming Rayleigh scattering can be written

$$a_A^* = \frac{a_A}{N} = \frac{1}{2.3} \frac{N_0}{N} k_m \alpha_i \quad s_A^* = \frac{s_A}{N} = \frac{1}{2.3} \frac{N_0}{N} \frac{k_m^4}{6\pi} (\alpha_r^2 + \alpha_i^2) \quad (9)$$

N_0 is Avogadro's number, k_m is the wavevector of light in the solution, and α_r and α_i are the real and imaginary parts of the polarizability of the aggregate. Since typical theories for the polarizability predict that the resonant part of α_r is zero at the maximum of S_A , the value of α_r should be quite small at this wavelength. Using the value of a_A^* and s_A^* at the peak of the S_A spectrum therefore allows for the assumption that $\alpha_r \ll \alpha_i$ and results in the following expression for N :

$$N = \frac{6\pi N_0 s_A^*}{2.3 k_m^2 (a_A^*)^2} \quad (10)$$

Using this expression on the data shown in Figure 7 yields a value for N of 320 000. Other H₄TPPS solutions with varying concentrations of porphyrin yield average aggregation numbers between this value and twice this value (see Table 1). Certainly these aggregates are quite large!

For some of the systems we have investigated, a large uncertainty is introduced into this calculation when the scattering component makes a relatively minor contribution to the extinction. In this case s_A^* is obtained from the subtraction of two large but similar numbers and is therefore subject to a large degree of uncertainty. The result is that the estimate of N is also quite uncertain. An alternative strategy for calculating N is to perform measurements both on the sample being investigated and on a "standard" for which N can be calculated as described above. If the wavelength, absorption, scattering, absorption coefficient in chromophore units, and angular factor for the sample are λ_X , A_X , S_X , s_X^* , and r_X , respectively, and if

the wavelength, absorption, scattering, absorption coefficient in chromophore units, angular factor, and aggregation number for the "standard" are λ_S , A_S , S_S , a_S^* , r_S , and N_S , respectively, then the aggregation number for the sample, N_X , is given by the ratios of these quantities:

$$N_X \approx \frac{\lambda_X^2 r_S a_X^* A_S S_X N_S}{\lambda_S^2 r_X a_X^* A_X S_S} \quad (11)$$

But since the scattering intensity as measured by the fluorimeter is nearly proportional to the scattering component of the extinction, the ratio S_X/S_S is approximately equal to I_X/I_S , where I_X and I_S are the fluorimeter intensities, corrected for absorption, for the sample and standard, respectively. The resulting relationship is therefore

$$N_X \approx \frac{\lambda_X^2 r_S a_S^* A_S I_X N_S}{\lambda_S^2 r_X a_X^* A_X I_S} \quad (12)$$

Of course, the sample and "standard" must be investigated using the same instrumental conditions (scattering geometry, slit width, wavelength resolution, etc.).

This ratio approach permits the estimation of the aggregation number without the necessity of parsing the extinction for the sample into its absorption and scattering components. We have tested this approach for cases in which a value of the aggregation number could be obtained via either method and the agreement is excellent. For those cases where only the ratio method was capable of producing good estimates, system-consistent values were obtained.

3.4. Angle-Dependent Light Scattering Experiments. The angular scattering measurements shown in Figure 6 can be used to estimate the size and shape of the aggregates, since these features of a scatterer determine the angular distribution of the scattered light. The analysis begins with a determination of which of three theoretical structure factors (that for a sphere, a Gaussian coil, or a thin rod) best fit the data.¹¹ Then by fitting this theoretical structure factor to the angle-dependent light scattering data, an estimate of the size and the shape of the scatterer can be determined. Least-squares fits for the scattering from a sphere and Gaussian coil do not approximate the H₄TPPS data at all. Shown in Figure 6 is the fit to the scattering data for a thin rod model, where it can be seen that the fit is fairly good and yields a length of about 0.6 μm . Since the distance between porphyrin molecules is about 0.35 nm if they are face to face, this would indicate an aggregation number of about 20 000 assuming the monomers form a linear array. While this number and the aggregation number determined from the extinction spectrum are both clearly estimates, they still are a useful description of the porphyrin assembly. A model consistent with all the data strongly suggests on the order of 10 000 monomers stacked face to face along the length of the aggregate and on the order of 20 monomers across its diameter. The lengths obtained from least-squares fits to a thin rod model for other concentrations of H₄TPPS are given in Table 1.

Several experiments were performed to make certain that the results were not adversely affected by the methods or equipment used. First, the wavelength scales of the spectrophotometer and fluorimeter were checked against each other by comparing the absorption spectrum of a narrow band-pass filter with the scattering spectrum of polystyrene spheres with the same filter in front of the detector of scattered light. A difference of 1 nm was found between the two instruments, so each fluorimeter

spectrum was shifted by 1 nm to take this difference into account. Second, ideally none of the light scattered by the sample in the spectrophotometer should reach the detector, even light scattered at very small angles. To check this, a small aperture was placed in front of both the reference and sample detectors to determine whether the "absorption" of a polystyrene sphere suspension would increase as less of the light scattered at small angles reached the detector in the sample path. No increase was observed, indicating that very little scattered light normally reaches the detector.

The shift of the scattering component peak to longer wavelength relative to the absorption component peak cannot be explained by classical absorption and scattering theory. There have been some indications of similar behavior in pseudoisocyanine chloride and thiocarbocyanine dyes,^{12,13} but the presence of overlapping fluorescent features makes the conclusions more problematic in those systems. One possible explanation for this red shift (which is unequivocal for the porphyrin system) lies with the energy level structure within the excited state band. If there are many more states near the lower edge of the band and if there is some redistribution of occupied states during the scattering process, then the distribution of scattered light could well shift to lower energy (i.e., longer wavelength). Continued investigation of this effect is planned.

Clearly the aggregation number, size, and shape of the H₄-TPPS aggregates, suggested by these experiments, are only estimates. Still, they provide information about these supramolecular assemblies that is extremely useful. First, these aggregates are quite large. Second, although these aggregates may have a linear structure, it does not appear that the cross-sectional area of these aggregates is due to a single monomer. Therefore, it should be kept in mind that simple models of these aggregates are probably not entirely accurate. Adding to the complexity of these systems is a good deal of evidence from our laboratory pointing to the fact that these aggregates also form an extremely weak network in solution (see the following section).

3.5. Dynamic Light Scattering Measurements. We have also measured the time autocorrelation function for H₄TPPS solutions in dynamic light scattering experiments. By measuring the relaxation time of the autocorrelation function under two polarization conditions, it is possible to measure the translational and rotational diffusion constants. Theoretical expressions for these diffusion constants have been worked out for several shapes. Perhaps the simplest example is the Kirkwood model of a long, thin rod with length L and diameter d .¹⁴ By comparing the experimental relaxation times with the theoretical expressions, L and d can be determined.² For the 3.71 μM H₄TPPS solution, the results are that $L \approx 0.8 \mu\text{m}$ and $d \approx 0.07 \mu\text{m}$. For other concentrations of H₄TPPS, the scattering intensity was too low in one polarization condition for this analysis to be useful. Instead, the hydrodynamic radius as measured with the other polarization condition is shown in Table 1.

It is interesting to note that the lengths as measured by both angular and dynamic light scattering experiments for the 3.71 μM H₄TPPS solution are not very different from each other. In addition, using the Kirkwood model for the diffusion of thin rods, the hydrodynamic radius of a thin rod should be less than its length by a factor of $[2 \ln(L/d)]^{-1}$. Using the results for L and d given above for the 3.71 μM solution, this theoretical factor turns out to be about 0.2, which is consistent with the experimental results for all four H₄TPPS solutions given in Table 1 considering the large error estimates for the hydrodynamic radii. Also of note is that an aggregate with about 20 monomers across its diameter would have a diameter of 0.04 μm , which

is on the same order as the estimate of the diameter from the dynamic light scattering experiments. It should be pointed out that the estimate of $d \approx 0.07 \mu\text{m}$ is very sensitive to the exact values of the two relaxation times, and therefore should be considered a very rough estimate.

Since the dynamic RLS measurements actually measure a hydrodynamic size, the results are very sensitive to any changes that affect how the aggregates diffuse through the solvent. One striking observation when performing such measurements on H₄TPPS solutions is that the relaxation times have a tendency to increase even when little change is observed in extinction and other scattering measurements. In fact, if the solution is shaken or stirred and a dynamic RLS experiment is done immediately, the measured relaxation times start out at a small but reproducible value and slowly increase over a period of an hour or so. The relaxation times return to their smaller values if the sample is shaken or stirred once again. This finding, along with other observations, indicates that the initial aggregation process is probably followed by an organization of the aggregates into some type of extremely weak network. This should be kept in mind, since some measurements are affected by the existence of this higher degree of organization much more than other measurements.

4. Conclusions

Resonance light scattering measurements have great potential for probing supramolecular assemblies of chromophores. With the use of this technique, however, comes a number of experimental complexities that must be sorted out before accurate quantitative information can be obtained. Chief among these complexities are (1) to determine how much of the extinction spectrum is due to absorption and how much is due to scattering, and (2) to correct the spectrum of scattered light to account for the effects of absorption on the instrumental results. A protocol involving specific measurements and careful analysis is capable of achieving these results, and these have been described in this article.

The results for the H₄TPPS system are quite revealing. Not only do the data imply important structural information, it is clear that the average size of the aggregates depends on the concentration of H₄TPPS. As is evident from Table 1, as the concentration of porphyrin increases, the size of the aggregates decreases. This could point to the fact that the average size of the aggregates depends more on the conditions during the early stage of aggregation (e.g., the density of aggregation nuclei) than on the equilibrium parameters of the system. Work on the kinetics of aggregate formation in the H₄TPPS system is ongoing in our laboratory.

Acknowledgment. This work was supported by National Science Foundation Grant CHE-9530707 and the Howard Hughes Medical Institute. We gratefully acknowledge useful conversations with Drs. Julio de Paula, Luigi Monsu' Scolaro, and Roberto Purrello.

References and Notes

- (1) Pasternack, R. F.; Bustamante, C.; Collings, P. J.; Giannetto, A.; Gibbs, E. J. *J. Am. Chem. Soc.* **1993**, *115*, 5393.
- (2) Pasternack, R. F.; Collings, P. J. *Science* **1995**, *269*, 935–939.
- (3) Pasternack, R. F.; Gurrieri, S.; Lauceri, R.; Purrello, R. *Inorg. Chim. Acta* **1996**, *246*, 7.
- (4) Parkash, J.; Robblee, J. H.; Agnew, J.; Gibbs, E.; Collings, P.; Pasternack, R. F.; de Paula, J. C. *Biophys. J.* **1998**, *74*, 2089.

- (5) Mallamace, F.; Micali, N.; Trusso, S.; Monsu Scolaro, L.; Romeo, A.; Terracina, A.; Pasternack, R. F. *Phys. Rev. Lett.* **1996**, *76*, 4741.
- (6) Fleisher, E. B.; Palmer, J. M.; Srivastava, T. S.; Chatterjee, A. *J. Am. Chem. Soc.* **1971**, *93*, 3162.
- (7) Tucker, S. A.; Amszi, V. L.; Acree, Jr, W. E. *J. Chem. Educ.* **1992**, *69*, A8.
- (8) Holland, J. F.; Teets, R. E.; Kelly, P. M.; Timnick, A. *Anal. Chem.* **1977**, *49*, 706.
- (9) Akins, D. L.; Zhu, H.-R.; Guo, C. *J. Phys. Chem.* **1994**, *98*, 3612.
- (10) Ribo, J. M.; Cusats, J.; Farrera, J.-A.; Valero, M. L. *J. Chem. Soc., Chem. Commun.* **1994**, 681.
- (11) Johnson, Jr., C. S.; Gabriel, D. A. *Laser Light Scattering*; Dover: New York, 1981; Chapter 1.
- (12) Fidler, H.; Terpstra, J.; Wiersma, D. A. *J. Chem. Phys.* **1991**, *94*, 6895.
- (13) Fidler, H.; Wiersma, D. A. *J. Phys. Chem.* **1993**, *97*, 11603.
- (14) Riseman, J.; Kirkwood, J. G. *J. Chem. Phys.* **1950**, *18*, 512.